Analysis of a New Variable-Speed Singly Salient Reluctance Motor Utilizing Only Two Transistor Switches

LONGYA XU, THOMAS A. LIPO, FELLOW, IEEE, AND SHEKAR C. RAO

Abstract—**A new type of two phase synchronous reluctance motor drive is introduced and analyzed. Since the currents in the phases are uni-directional rather than bidirectional, the associated power converter requires only two transistors and two feedback diodes. It is demonstrated by the finite element method of analysis that with the same amount of active copper and under the same rated power output, the copper losses of this machine can be reduced to 75% of that of the equivalent switched reluctance motor.**

INTRODUCTION

ALTHOUGH induction motor drives are still the workhorse of industry, the switched reluctance (SR) motor drive has been actively researched over the past decade with very promising results [1]–[3]. The SR machine has a simple and rugged construction as well as very good overall performance over a wide torque-speed range [2]. Recently, doubly salient switched reluctance motors have been found to be an attractive alternative to more conventional PM synchronous and induction machines in low horsepower, converter fed variable-speed drive applications.

Since the current waveform of this motor must be carefully programmed to extract the maximum torque/ampere, this machine is more accurately termed a current regulated stepping motor or simply a CRS motor [4]. The fundamental feature of this type of motor drive is that the CRS motor requires only a unidirectional current and thus the circuit topology and corresponding switching algorithm is greatly simplified. A detailed comparison of the CRS motor drive with a high efficiency induction motor drive has indicated that performance parameters, such as torque per unit stator volume, torque per unit inertia and torque per unit copper weight, can be made equal to that of an induction machine, or, in some cases, even exceed the induction machine [3].

While the recent work on CRS machines are encouraging, the jury is still out on whether the machine is truly an optimum geometry. In several respects the machine is clearly suspect. For example, taking a 8 stator/6 rotor pole CRS motor as an illustration, with typical excitation of one of the four phases, only one quarter of the stator inner circumference is utilized to make a contribution to torque development at any instant. Secondly, the inductance variation of the occupying coils over each one fourth of the machine is limited by the so called double salient design. In order to have a comparable power rating to that of the conventional induction machine of the same size with such a limited airgap inner surface area the CRS is designed to operate in a deeply saturated condition. The corresponding active material thus is under severe electromagnetic stress. It is apparent that any method of ensuring that the other three quarters of the inner circumference of the stator remain active will be a very significant step towards improving torque production and, therefore, towards relaxing the severe electromagnetic stress and consequent iron losses in the active materials of the machine.

This paper describes and analyzes a new type of synchronous reluctance motor utilizing concentrated windings, an axially laminated rotor, and unidirectional winding currents which shows promise in outperforming the CRS motor. The paper proposes that with the same active air gap surface, and same amount of active copper at the rated output power, the copper losses of the machine can be dropped to 75% and, under 140% rated output power, to 55% that of its CRS motor counterpart. The feasible improvement of copper losses in a synchronous reluctance motor can be attributed to the full pitch coils in each phase and to a segmented rotor construction which ensure that the entire airgap surface remains active. Since the entire airgap is active during any interval of the torque production period, the corresponding active materials can work more efficiently under relatively mild electromagnetic stress. Because this machine also requires careful regulation of the stator current to extract maximum torque, the machine is denoted in this paper as a current regulated reluctance motor or current regulated reluctance (CRR) motor.

Based on the concepts presented in this paper, a compatible number of stator phases and rotor poles are chosen for both the CRS and CRR motors with the same frame size and the torque production and copper losses are analyzed and compared both by idealized analysis and by the finite element method.

REVIEW OF TORQUE PRODUCTION IN A CRS MOTOR

Electromechanical energy conversion in a CRS motor, shown in idealized form in Fig. 1, is accomplished by means of a time varying inductance due to the temporal variation of the rotor position. This principle can be best illustrated by

Paper IPCSD 89-39, approved by the Electric Machines Committee of the IEEE Industry Applications Society for presentation at the 1988 Industry Applications Society Annual Meeting, Pittsburgh, PA, October 2-7. Manuscript released for publication August 14, 1989.

L. Xu and T. A. Lipo are with the Department of Electrical and Computer Engineering, University of Wisconsin, Madison, WI 53706.

S. C. Rao is with Kurz and Root Company, Appleton, WI 54915.

IEEE Log Number 8932120.

0093-9994/90/0300-0229$01.00

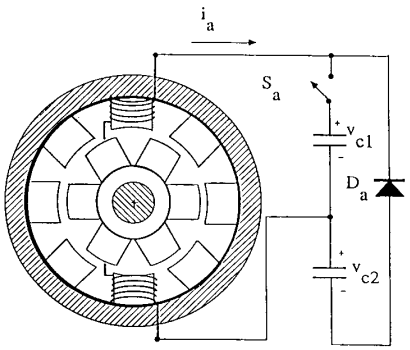

Fig. 1. Idealized representation of eight pole stator-six pole rotor switched reluctance current regulated stepping (CRS) motor.

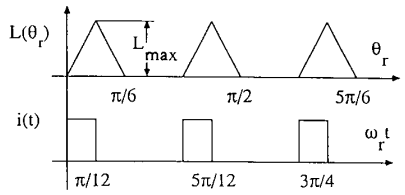

Fig. 2. Inductance variation and current profile for one of phases of 8/6 pole CRS motor.

plotting a typical stator winding inductance profile versus rotor position with respect to the winding axis together with the corresponding stator current waveform as shown in Fig. 2. It should be noted that the plots are idealized and the current is assumed to flow only during the interval when motoring torque production is possible.

For simplicity of analysis, all the losses and saturation are temporarily neglected. The voltage induced in the winding is

$$E = \frac{d\lambda}{dt} = L\frac{di}{dt} + i\frac{dL}{d\theta_r}\frac{d\theta_r}{dt} \tag{1}$$

where L is only a function of rotor angular displacement (saturation neglected).

The instantaneous power entering the circuit is

$$P = Li\frac{di}{dt} + i^2\frac{dL}{d\theta_r}\omega \tag{2}$$

where the rotor angular speed $d\theta_r/dt$ is assumed to be a constant, ω. Equation (2) can be further written in the form

$$P = \frac{1}{2}L\frac{di^2}{dt} + \omega i^2\frac{dL}{d\theta_r} + \frac{1}{2}i^2\frac{dL}{dt} - \frac{1}{2}i^2\frac{dL}{d\theta_r}\frac{d\theta_r}{dt} = \frac{d}{dt}\left[\frac{1}{2}Li^2\right] + \frac{1}{2}i^2\frac{dL}{d\theta_r}\omega. \tag{3}$$

Equation (3) yields the well known result that the input electrical power is equal to the derivative of the stored field energy and the mechanical output power. The second term in the right hand side of (3) indicates that the electromagnetic torque can be expressed as

$$T = \frac{1}{2}i^2\frac{dL}{d\theta_r}. \tag{4}$$

By examining (4), the following conclusions can be reached immediately.

1) Motoring torque is produced if the CRS machine is excited during the interval in which the inductance of the winding is increasing, that is, when $dL/d\theta_r$ is positive.
2) Generating torque is produced if CRS machine is excited during the interval in which the inductance of the winding is decreasing, that is, when $dL/d\theta_r$ is negative.
3) Torque production is proportional to the square of the current and therefore independent of current polarity if mutual inductance is not involved. Hence, the windings can be excited with unidirectional currents.
4) To maximize the torque for a given current $dL/d\theta_r$ should be maximized.

From a motor design point of view, 4) implies that within a fixed angle of rotor rotation, the stator winding inductance difference should be as large as possible.

The limitation imposed by a CRS motor in maximizing $dL/d\theta_r$ can be explained by taking a two pole rotor and one phase stator coil CRS motor as an example, as illustrated in Fig. 3. In order to maximize L_{max}, the stator pole should be completely aligned with the rotor pole. On the other hand, to minimize L_{min} the stator pole should be totally nonaligned with the rotor pole. Therefore, a design constraint exists wherein the relationship

$$\beta_s + \beta_r \leq 2\pi/N_r \tag{5}$$

must be satisfied where N_r is the number of rotor poles. Under this constraint, L_{min} is limited by the leakage flux and L_{max} is limited by the permeance of the main flux path which is set by the cross-section of the stator pole and minimum allowable air gap. In general, these limitations generally result in a maximum achievable ratio of L_{max}/L_{min} of 10:1 when saturation is neglected. Another limitation, set by the small working area of the double salient structure, is that the permeability of cross-section is strongly affected by the excitation level which is detrimental to the maximizing the ratio of L_{max}/L_{min}. It is therefore clear that a marked improvement in $dL/d\theta_r$ is not practical without increasing the number of poles (reducing $\Delta\theta_r$) which, unfortunately, reduces the power output of the machine, or conversely, to very high switching frequencies in the associated power converter. Nevertheless, the analysis of the CRS motor gives us a clue to exploring partial improvements of the term $dL/d\theta_r$ in the torque equation.

Basic CRR Motor Configuration

The rotor structure of the CRR motor presented in this paper is depicted in Fig. 4. For a six pole CRR machine, which is the equivalent of the 8 pole stator/6 pole rotor stepping mo-

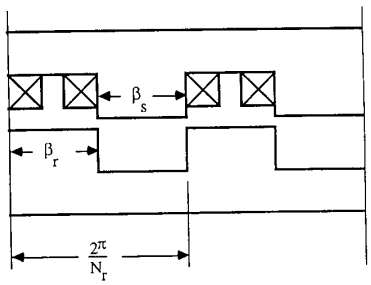

Fig. 3. Illustrating design limitation of doubly salient construction.

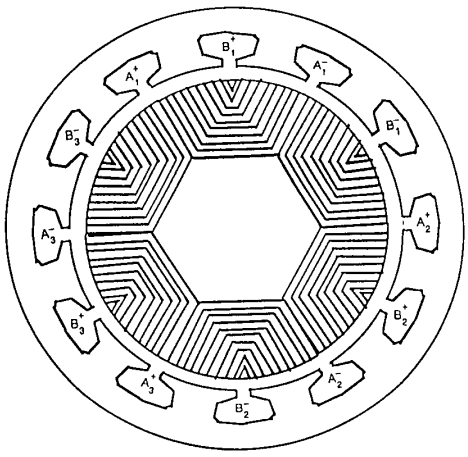

Fig. 4. Rotor and stator assembly of six pole CRR motor showing segmented rotor structure with axial laminations.

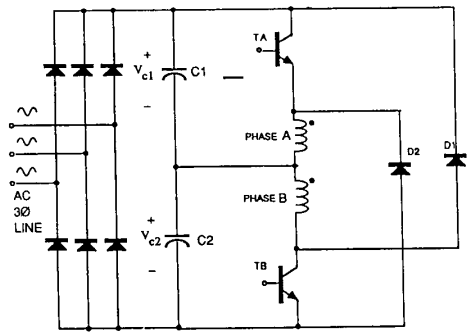

Fig. 5. Power converter for CRR motor utilizing only two transistor switches.

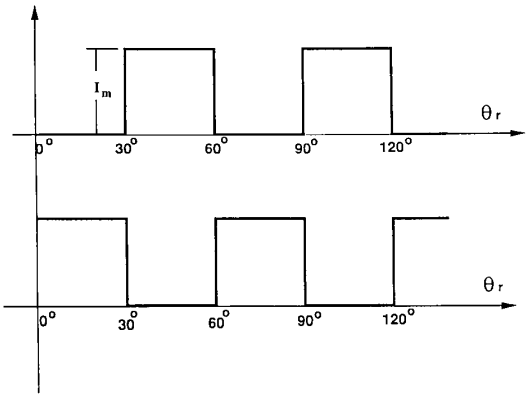

Fig. 6. Current wave shape of the two phase CRR motor as function of rotor position.

tor, the rotor is divided into six segments, and each segments consists of a stack of axially laminated iron sheets sandwiched with nonmagnetic material [6]. The rotor is then fitted into a stator having fully pitched windings. The function of the axially laminated rotor is to create as large a saliency as possible in terms of $\Delta L = L_{\max} - L_{\min}$. The type of machine is, of course, not restricted to axially laminated structure and other types of rotor geometries resulting in a large value of $\Delta L/\Delta\theta$ are equivalently suitable for this purpose. To better distribute the load current around the stator periphery, the machine can be designed with any number of phases. However, a two phase CRR machine is most analogous to the 8/6 pole CRS motor and results in the lowest losses. The phases are designed to carry unidirectional currents in the same manner as the CRS machine.

Several converter arrangements are possible to power this machine [1], [2], [7]. One of the simplest uses a split dc bus and only two transistors, as shown in Fig. 5. The currents are, in effect, unidirectional blocks of current with a duration of 90 electrical degrees and occurs with two pulses per cycle as shown in Fig. 6. Since the flux in each coil is a pulsing dc quantity, the rotor poles encounter an ac flux variation during a complete rotation. Because the rotor poles are not polarized, a continuous unidirectional torque can still be maintained and, excluding stationary effects and, assuming ideal switching of the currents, the torque is a non-pulsating quantity.

Comparison of Torque Capability of CRS and CRR Motors

Prototype CRS and CRR motors are shown in Figs. 1 and 4. For the purpose of comparison, the following assumptions are made.

1) The two motors have the same stator inner diameter, the same length of the iron stack and the same length of airgap.

2) The number of rotor poles are the same for both motors.

3) Both motors have the same total number of turns of stator windings and the wire gauge is the same and therefore the two machines have the same amount of active copper weight.

4) Each stator phase winding has the same current and because of 3), the same current density.

5) The CRS machine has 4 stator coils and CRR motor 6.

6) The magnetic materials in both motors work in the linear region.

7) Consistent with manufacturing experience, the ratio $L_{\max}/L_{\min}$ is assumed to be 10 and 5 for the CRS motor and CRR motor respectively.

Based on assumptions 1) through 6) it immediately follows that the turns per coil and MMF produced by a coil in a two phase, six pole CRR motor is 2/3 of that in a four phase, eight pole CRS motor. The flux density in a CRR motor is thus 2/3 of that in a CRS motor. Because both motors have the same number of rotor poles, each coil in both the CRS and CRR motors is excited six times for each revolution of the rotor.

The period for excitation of each coil in a CRS motor is 15 degrees. However, for a coil in a CRR motor it is 30 degrees.

It can be recalled that the instantaneous torque during the period of excitation of any coil is governed by (5). For convenience, it will be assumed that during the excitation period the coil inductance is a linear function of rotor position θ_r. Then (5) can be written in the form:

$$T = \frac{1}{2} i^2 \frac{L_{\max} - L_{\min}}{\Delta\theta_r} \tag{6}$$

where $L_{\max}$ and $L_{\min}$ are the inductances in the maximum and minimum inductance positions respectively and $\Delta\theta_r$ is the swept rotor angle over which this inductance variation takes place.

It is convenient to let

$$k_L = 1 - \frac{1}{L_{\max}/L_{\min}} \tag{7}$$

The torque can then be written as

$$T = \frac{1}{2} i^2 \frac{k_L L_{\max}}{\Delta\theta_r} \tag{8}$$

It can be recalled that the inductance can be expressed as [8]

$$L_{\max} = \frac{\mu_0 l r \theta_0 N^2}{2g} \tag{9}$$

where

- μ_0 permeability of air,
- l length of the stack,
- r radius of the rotor,
- θ_0 overlapped pole arc between one stator and rotor pole when each current interval ends,
- g length of airgap,
- N # of turns per coil.

Substituting (10) into (9), the average torque contributed by a singe coil in one rotor revolution is therefore

$$T_{(\text{ave})} = \frac{3}{\pi} \left[\frac{1}{2} i^2 \frac{k_L \mu_0 l r \theta_0 N^2}{2g} \right]. \tag{10}$$

It is important to note the difference between the instantaneous torque and the average torque which is independent of the incremental rotor angle $\Delta\theta_r$. Taking the number of phases and number of circuits per phase into account, the total average torque produced by the machine is

$$T_{(\text{ave})} = mC \left[\frac{3}{2\pi} i^2 \frac{k_L \mu_0 l r \theta_0 N^2}{2g} \right] \tag{11}$$

where

- m number of phases,
- C number of circuits per phase.

For purposes of comparison, it is convenient to simply denote all quantities associated with CRS motor by the subscript 1 and those of the CRR motor by 2. Therefore, a torque ratio expressing the degree of improvement of the CRR motor relative to the CRS motor can be written as

$$\tau = \frac{T_{2\,(\text{ave})}}{T_{1\,(\text{ave})}} = \frac{m_2 C_2 k_{L_2} \theta_{0_2} N_2^2}{m_1 C_1 k_{L_1} \theta_{0_1} N_1^2} \tag{12}$$

where we have already made use of the fact that $i_1 = i_2$.

This expression clearly indicates the importance of the iron cross-sectional area spanned the coil i.e., the importance of θ_o. From assumptions 1) through 7), we have

$$N_2 = 0.67N, \qquad N_1 = N,$$
$$m_2 = 2, \qquad m_1 = 4,$$
$$C_2 = 3, \qquad C_1 = 1,$$
$$k_{L2} = 4/5, \qquad k_{L1} = 9/10,$$
$$\theta_{o2} = 60^\circ \qquad \theta_{o1} = 18^\circ.$$

Upon evaluation of (12) using the above parameters, the torque ratio between the CRR motor and CRS motor becomes

$$\tau = 1.997. \tag{13}$$

Hence, with the identical frame size and active copper weight, the CRR motor will develop as twice as much torque as that of the CRS motor. That is, the power density of a CRR motor will be twice that of a CRS motor.

It is important to note that the improvement in output torque does not come without a commensurate increase in the copper losses. Since the pole pitch of each stator winding embraces one sixth of the stator inner circumference, the end winding portion of the windings of the CRR machine are proportionately larger, contributing, in turn, to higher copper losses. A sketch of the coils geometry of the windings for the two machines are shown in Fig. 7. It can be readily verified that the ratio of the resistances for the two machines can be expressed as

$$\frac{R_2}{R_1} = \frac{2\left(L + \frac{\pi}{6} r\right)}{L + \frac{\pi}{10} r} \tag{14}$$

where L is the length of the coil in the axial direction. For a machine rated at 7.5 kW (Table I) the ratio of resistance of the CRR to CRS machine can be shown to be

$$R_2/R_1 = 2.2. \tag{15}$$

Hence, for the same current in the windings of the two machines, the torque of the CRR machine is double that of the CRS machine. However, the copper losses increase as well by a factor of 2.2. In general, this ratio typically takes values from 2.0 to 2.5 depending upon the aspect ratio. Therefore, while the new machine is capable of high power density, it appears that the CRR motor is not more efficient than the CRS machine. It should be remembered, however, saturation has, to this point, been neglected. It can be recalled that to extract a practical amount of power from the stepping (CRS) motor, the machine must be driven deeply into saturation. Hence, the

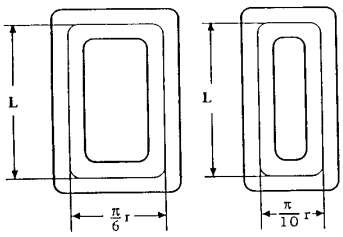

Fig. 7. Coil geometry for CRS and CRR motors.

TABLE I
PARAMETERS OF THE COMMERCIALLY DESIGNED MOTOR

	Outer diameter of stator lamination 204.8 mm
Stator Poles 8	Inner diameter of stator lamination 116.8 mm
Rotor Poles 6	Airgap 0.35 mm
Horsepower 7.5/10 kW	Length of stator lamination 171 mm
Voltage 380/418 V	
Current 16A	

preliminary results of the present section must be reexamined in light of saturation effects.

Finite Element Analysis

Although the linear model used previously has provided some insight to understanding of the principles of the reluctance machines, to properly evaluate and compare the design and performance of the CRS and CRR motors, more reliable models are required. Hence, the finite element method (FEM) has been utilized. The magnetic field of both CRS and CRR geometry was described in a descretized model and solved by the FEM. The solutions were obtained from a FEM package developed at the University of Wisconsin. Again the assumptions of the previous section were used so that the machines have the same active copper, and air gap surface area. The 8/6 pole CRS and 6 pole CRR motors were again compared. The $B-H$ curve for mild steel was used in the computation.

Due to the complicated geometry of the motors and the small size of the airgap (0.35 mm), the size and shape of each element of the solution must be carefully determined. Hence, approximately 3500 elements were generated for the CRS and 2000 for CRR motor which ensures relatively high accuracy for the solutions. In order to evaluate the flux linkage variation and torque capability in terms of rate of coenergy variation with respect to the rotor position, the field plots for numerous different rotor positions were obtained.

Figs. 8 and 9 show vector potential lines (flux lines) for two typical rotor positions for the CRS machine. Similar plots are given in Figs. 10 and 11 for the CRR motor. These four plots provide a good descriptive picture of flux distribution for the CRS and CRR motors. In addition, the regions of local saturation can be spotted easily by inspection.

Figs. 12 and 13 show a families of flux linkage-current curves for the CRS and CRR motors respectively at various rotor positions obtained from 120 finite element plots. These curves show the bulk saturation effect of the two motors. It is important to note that these two motors saturate at quite

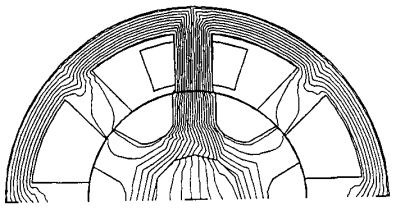

Fig. 8. Finite element plot of flux distribution of CRS motor for typical aligned position.

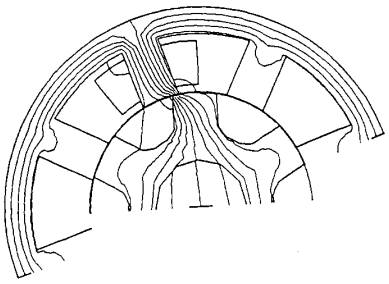

Fig. 9. Finite element plot of flux distribution of CRS motor for typical unaligned position.

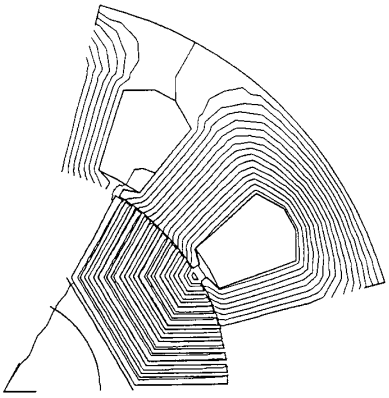

Fig. 10. Finite element plot of flux distribution of CRR motor for typical aligned position.

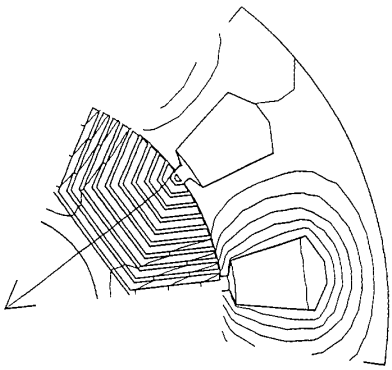

Fig. 11. Finite element plot of flux distribution of CRR motor for typical unaligned position.

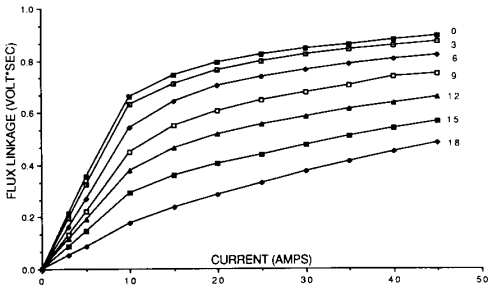

Fig. 12. Flux link versus current curves for 8/6 pole current regulated stepping motor (CRSM).

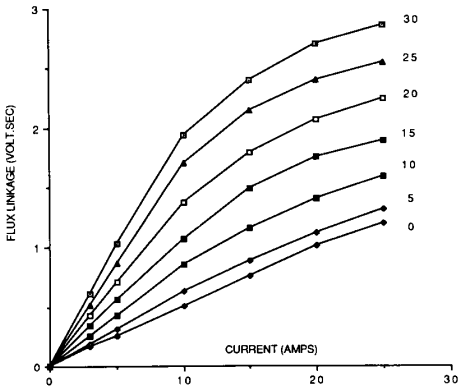

Fig. 13. Flux linkage versus current curves for 6 pole current regulated reluctance motor (CRRM).

different flux linkage levels. Also the flux linkage variation with respect to the rotor positions at the same excitation level are different. These two curves are very significant for predicting the induced speed voltages for a given current thus to establish the torque production of the machine. For example, at 10 A excitation level, the variation of flux linkage $\Delta\lambda$ of CRR for $\Delta\theta_r = 15°$ (0°-15°) is 0.85 volt seconds, while the $\Delta\lambda$ of CRS for $\Delta\theta_r = 15°$ (3°–18°) is 0.43. At higher excitation level, 25A, the variation of flux linkage $\Delta\lambda$ of CRR for $\Delta\theta_r = 15°$ (0°–15°) is 1 volt seconds, while the $\Delta\lambda$ of CRS for $\Delta\theta_r = 15°$ (3°–18°) is 0.46 due to the deep saturation.

The average torque production is evaluated by calculating the rate of coenergy variation due to the rotor rotation, that is,

$$T_{(\text{ave})} = \frac{\Delta E}{\Delta\theta_r}\Big|_{I=\text{const}} \tag{14}$$

where ΔE is the coenergy variation corresponding to the variation of rotor angle displacement $\Delta\theta_r$ in mechanical degrees under constant excitation current. The angular displacement $\Delta\theta_r$ for the CRS motor is from 0 to 18 mechanical degrees as shown in Fig. 12 and for the CRR motor is from 0 to 30 mechanical degrees as shown in Fig. 13.

The current-torque relations, computed from Figs. 12 and 13 are plotted in Figs. 14 and 15. In computing Figs. 14 and 15 it was assumed that the motor currents retain their ideal waveform illustrated in Figs. 2 and 6. In contrast to the linear model in which the torque derived is proportional to the square

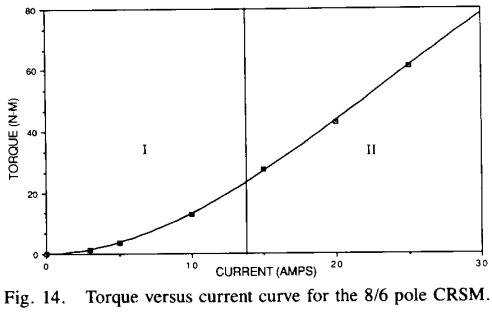

Fig. 14. Torque versus current curve for the 8/6 pole CRSM.

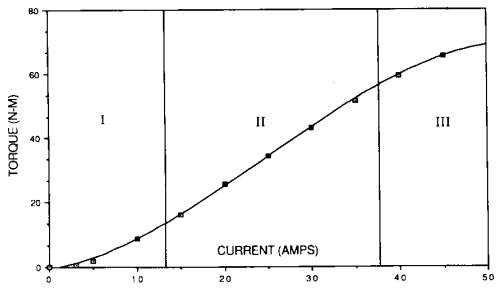

Fig. 15. Torque versus current curve for the 6 pole CRRM.

of the current, the computed torque capability can be divided into three regions depending on the excitation level. Taking the current-torque curve for the CRS motor as an example, in Region I (relatively unsaturated) the torque is indeed proportional to the square of the current. However, in the middle region II the torque is only linearly proportional to the current because the iron of the motor has entered the saturation region but the flux is still well confined by the path provided by the rotor iron. In the last Region III, not only is the iron deeply saturated but also the flux linkage does not follow the path provided by the rotor iron and the leakage flux becomes dominant. Under such circumstances, the flux linkage varies in less than a linear fashion and, consequently, so does the torque production. Note from Fig. 14 that for a given torque the CRR motor remains far less saturated than the CRS motor, suggesting an increased torque per ampere. It is apparent that the saturation of reluctance type motors are crucial to the overall performance and must be adjusted correctly.

Experimental Results

To verify the accuracy of the nonlinear CRR and CRS motor models established by finite element method analysis, an experimental CRR motor was built and tested. This prototype CRR motor is constructed with four poles, instead of six poles as discussed previously, and fit into a frame of a standard induction motor. An identical FEM approach used in the analysis of 6-pole CRR and CRS motors was applied for the theoretical prediction of the 4-pole prototype motor. For the same range of the current and rotor positions, the average torque capability of the 4-pole CRR motor was calculated and tested. The predicted and measured torque per ampere of this machine is shown in Fig. 16 and reasonably good agreement between the calculated and experimental results is clearly evident.

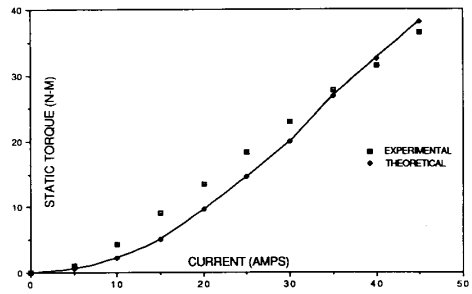

Fig. 16. Theoretical and experimental torque production of 4-pole CRR motor.

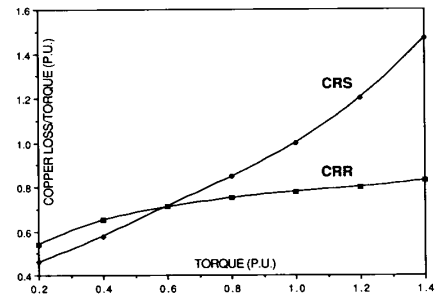

Fig. 17. Copper loss/torque ratio versus per unit electromagnetic torque.

Performance Comparison of CRS and CRR Motors

It is well known that the CRS motor is a type of copper-loss dominant motor. Since the copper losses are proportional to the square of the current then, as in any good motor design, the motor should operate in a current versus torque region such as the ratio of copper-loss/torque is near its lowest possible value. Since both the CRS and CRR motors are assumed have the same physical size and operating speed, it is reasonable to take the ratio of copper losses to torque as a criterion and evaluate this parameter at various torque values for comparison. Using the torque production curves obtained by FEM, the ratio I^2R/T_e can be calculated and normalized by the rated value of the CRS motor for both motors where I^2R is the total copper losses and T_e is the corresponding electromagnetic torque. The resultant I^2R/T_e curves for the commercially available CRS motor and the experimental CRR motor are obtained and plotted in Fig. 17. The parameters of the commercially designed motor is given in Table I. The torque range evaluated from 0.2 to 1.4 times that of the rated torque of the CRS motor. It is clear that at low output torque levels the copper losses of the CRR motor are slightly higher than that of the CRS motor as also predicted by the linear analysis of the previous section. At a medium torque level, however, the difference between the CRS and CRR machines becomes evident. At the rated torque value the copper losses of CRR is 75% and at 140% rated torque is 55% of that of the CRS motor. Hence, with essentially the identical frame size and active copper weight, the CRR motor will have a higher efficiency than that of CRS motor under the rated power condition. This result may be interpreted in an alternative way. That is, if the copper losses of the CRS and CRR motors are the same, the CRR motor will then develop more torque than the CRS motor.

This conclusion can also be understood by inspection of the CRS and CRR motor operation physically. It should be noted in particular that during each energy conversion period, the CRS only has one quarter of the inner circumference of the stator making a contribution to torque production. As the current increases, the output power increases and so does the copper losses. However, when the CRS motor is at high power levels, the copper losses continue increasing proportional to the square of the current while the increase of the torque production is dramatically reduced by the iron saturation. The CRR motor, with its dedicated rotor and stator design, results in the entire airgap surface being active under very mild electromagnetic stress on the corresponding materials even at relatively high output power level. Therefore, it is not surprising that for medium power levels and above, the CRR motor converts energy more efficiently, or, for the same amount of copper losses, the CRR will convert more energy for the same rotor speed.

Although the CRR motor has significantly reduced copper losses per unit torque with the same physical size at or above the rated power level, the flux distribution in the machine still retains desirable characteristics. First, the magnitude of the flux density is dramatically reduced since the MMF is distributed along the entire airgap circumference. Secondly, the fundamental frequency of the variation of the flux pattern is reduced to one half that in the CRS motor since for each 60 degrees of rotor rotation the converter switches only two times instead of four times as in the equivalent CRS motor. The reduction of both magnitude and frequency of the flux variation in CRR motor should serve to decrease the iron losses of the machine.

Other advantages of the new current regulated reluctance motor are as follows.

1) With proper control, the two phase motor can develop starting torque of either polarity and rotate in either direction. This is in contrast to a two phase (four pole stator/two pole rotor) CRS motor which is well known to be incapable of developing reliable starting torque.
2) While a two pole rotor CRS motor will not develop starting torque, a two phase CRR motor can be designed with any (even) number of poles. Hence, this new machine offers improved high speed,high horsepower capability due to the low ratio of switching frequency to rotor speed.
3) Since only two phases are required, the motor requires only two self commutated switches in the power converter. This is in contrast to the CRS motor which typically requires 4 switches for a four phase 8/6 pole design or 6 switches for a three phase 6/4 pole design.
4) Since the switching frequency is reduced by half compared to an equivalent CRS motor with the same number of rotor poles, iron losses associated with the switching frequency are reduced.
5) Since the flux density in the rotor is almost entirely in the plane of the lamination and also normal to the axial direction, the rotor can be constructed with grain-oriented steel thereby further contributing to a reduction in the iron losses.

Conclusion

This paper has presented a new type of reluctance motor based on a salient pole rotor but with a cylindrical stator geometry. The windings are excited by a set of two unidirectional currents thereby affording the use of a simple two transistor power converter. This new class of reluctance machine appears to offer reduced losses compared to an equivalent switched reluctance (current regulated stepping) motor. While only two phase unidirectional stator currents have been considered in this paper, it is clear that the current amplitude of a similar machine with bidirectional currents would be halved for the same flux variation. Other numbers of phases with either unidirectional (pulsating) or alternating currents are clearly feasible and are presently under investigation.

Acknowledgment

This work was sponsored by the industrial members of the Wisconsin Electric Machines and Power Electronic Consortium (WEMPEC) to whom the authors are greatly indebted. The authors also thank the Bogue Electric Manufacturing Co., Paterson, NJ for constructing, to our specifications, the special uncast rotor used in the experimental study.

References

[1] P. J. Lawrenson, J. M. Stephenson, P. T. Blenkinsop, J. Corda, and N. N. Fulton, "Variable-speed switched reluctance motors," in *Proc. Inst. Elec. Eng.*, vol. 127, July 1980, pp. 253–265.

[2] W. F. Ray, P. J. Lawrenson, R. M. Davis, J. M. Stephenson, N. N. Fulton, and R. J. Blake, "High performance switched reluctance brushless drives," *IEEE Trans. Ind. Appl.*, vol. IA-22, no. 4, pp. 722–729, July/Aug. 1986.

[3] M. R. Harris, J. W. Finch, J. A. Mallick, and T. J. E. Miller, "A review of the integral horsepower switched reluctance drive," *IEEE Trans. Ind. Appl.*, vol. IA-22, pp. 716–721, July/Aug. 1986.

[4] T. A. Lipo and L. Y. Xu, "A novel converter fed reluctance motor with high power density," *Symposium on Electric Drives*, Cagliari, Italy, June 1987, pp. 315–321.

[5] A. R. W. Broadway, "Cageless induction machine," in *IEE Proc.*, vol. 118, no. 11, November 1971, pp. 1593–1600.

[6] S. C. Rao, "AC synchronous motor having an axially laminated rotor," U.S. Patent 4 110 646, Aug. 29, 1978 (Bogue Electric Assignee).

[7] J. T. Bass, T. J. E. Miller, M. Ehsani, and R. L. Steigerwald, "Development of a unipolar converter for variable reluctance motor drives," in *Conf. Rec. IEEE/IAS Annual Meeting*, 1985, pp. 1062–1068.

[8] N. L. Schmitz and D. W. Novotny, *Introductory Electromechanics*. New York: Ronald, 1965.

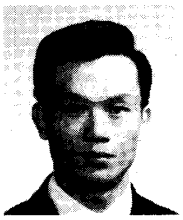

Longya Xu was born in Hunan Province, People's Republic of China. He graduated from Shangtan Institute of Electrical Engineering in 1970. He received the B.E.E. degree from Hunan University, Hunan, China, and the M.S. degree from the University of Wisconsin-Madison, in 1982 and 1986, respectively.

He is currently a Ph.D. Student in the Department of ECE, University of Wisconsin-Madison. From 1971–1978 he participated in the 120-kW synchronous machine design, manufacturing, and testing in China. From 1982–1984, he worked as Researcher for the linear electric machine in the Institute of Electrical Engineering Sinica Academia of China. Since 1984, he has been a Teaching and Research Assistant at the University of Wisconsin-Madison. His area of interests includes power electronics and converter optimized electrical machine, design, modeling, and simulation.

Thomas A. Lipo (M'64–SM'71–F'87), for a photograph and biography, please see page 221 of this TRANSACTIONS.

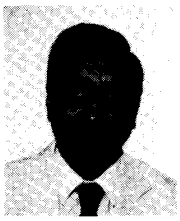

Shekar C. Rao received the M.S. degree in applied physics and electrical engineering from the Newark College of Engineering.

He is presently Vice President of Engineering at the Kurz and Root Company, Appleton, WI. He has made significant contributions in the field of electric machines, particularly in high frequency applications, holding several patents. His concepts on variable speed constant frequency generators led to a research and development contract for the development of windmill generators for NASA.

Mr. Rao is a member of the Synchronous Machinery Subcommittee and the Rotating Machinery Subcommittee of IAS.